



# An alternative cooling system to enhance the safety of Li-ion battery packs

Riza Kizilel<sup>a</sup>, Rami Sabbah<sup>a</sup>, J. Robert Selman<sup>a,b</sup>, Said Al-Hallaj<sup>b,\*</sup>

<sup>a</sup> Department of Chemical and Biological Engineering, Illinois Institute of Technology, 10 W. 33rd Street, Chicago, IL 60616, United States

<sup>b</sup> All Cell Technologies, LLC, IIT University Technology Park, 3440 S. Dearborn Street, Suite 117N, Chicago, IL 60616, United States

## ARTICLE INFO

### Article history:

Received 28 March 2009

Received in revised form 19 June 2009

Accepted 22 June 2009

Available online 30 June 2009

### Keywords:

Li-ion batteries

Thermal management

Thermal runaway

Phase change material

PCM

Li-ion battery safety

## ABSTRACT

A passive thermal management system is evaluated for high-power Li-ion packs under stressful or abusive conditions, and compared with a purely air-cooling mode under normal and abuse conditions. A compact and properly designed passive thermal management system utilizing phase change material (PCM) provides faster heat dissipation than active cooling during high pulse power discharges while preserving sufficiently uniform cell temperature to ensure the desirable cycle life for the pack. This study investigates how passive cooling with PCM contributes to preventing the propagation of thermal runaway in a single cell or adjacent cells due to a cell catastrophic failure. Its effectiveness is compared with that of active cooling by forced air flow or natural convection using the same compact module and pack configuration corresponding to the PCM matrix technology. The effects of nickel tabs and spacing between the cells were also studied.

© 2009 Elsevier B.V. All rights reserved.

## 1. Introduction

A lithium-ion (Li-ion) battery pack would be potentially more compact as well as light compared to a nickel metal hydride (NiMH) battery pack. Besides, they provide superior power capability compared. Hence, Li-ion batteries are used to replace the Ni-based batteries in the power tool industry and are also considered to be the preferred choice of battery for the next generation hybrid vehicles (HEV), and electric vehicles (EVs). However, compactness of Li-ion battery packs gives rise to safety issues due to potential overheating [1]. It is well known that under normal power/current loads and ambient operating conditions, the temperature within most Li-ion cells can be easily controlled to remain in the range of 20–55 °C. However, stressful conditions such as high power draw at high cell/ambient temperatures, as well as defects in individual cells, may steeply increase local heat generation. This may lead to thermal runaway of some cells and propagation of excessive temperature throughout a module or pack. Therefore, a thermal management system must prevent such propagation, without over-designing the cooling system and complicating control of battery performance [2].

A robust battery thermal management solution using PCM has been presented and demonstrated by our research group [3–7]. The technology provides a compact and simple design for controlling battery temperature in Li-ion technology. Initial analysis and exper-

iments on high energy Li-ion cells have shown that under normal operating conditions the graphite–PCM matrix keeps the temperatures of individual cells in a favorable range, similar to that achieved by air-cooling, with very good uniformity from cell to cell [6]. Moreover, if the module or pack is operated under stressful conditions, such as high current draw and high ambient temperature, the individual cells are kept at a lower and more uniform temperature than is possible by air-cooling [7]. This is ensured by the heat absorption due to phase change, if the melting point range of the PCM is properly chosen.

In this study, the potential of the passive thermal management is evaluated for high-power Li-ion packs under abuse conditions and compared with the air-cooling system. The study encompasses possible methods to accomplish sufficient heat dissipation in a compact geometry, while preserving sufficiently uniform cell temperature to ensure adequate cycle life for the module or pack. The results presented in this study also suggest that passive cooling by PCM may be an efficient and essential contribution to preventing the propagation of thermal runaway. Its effectiveness is comparable and sometimes better than that of active cooling (by forced air flow or natural convection), while not compromising the compactness of the pack.

## 2. Battery design

This study considers a high-power Li-ion battery pack suitable for plug in hybrid electric vehicle (PHEV) application. It is specifically designed for a Ford Escape Hybrid in order to replace the existing NiMH battery pack. A battery pack of this type is being

\* Corresponding author. Tel.: +1 312 235 3705; fax: +1 312 235 3703.

E-mail address: [salhallaj@allcelltech.com](mailto:salhallaj@allcelltech.com) (S. Al-Hallaj).

### Nomenclature

$C_p$	heat capacity of the cell ( $\text{J kg}^{-1} \text{K}^{-1}$ )
$h$	heat transfer coefficient ( $\text{W m}^{-2} \text{K}^{-1}$ )
$k$	thermal conductivity of the cell ( $\text{W m}^{-1} \text{K}^{-1}$ )
$Q(t)$	heat generation term during discharge or thermal runaway ( $\text{W m}^{-3}$ )
$T$	temperature of the cell (K)
$\rho$	density of the cell ( $\text{kg m}^{-3}$ )

### Subscripts

$c$	cell
PCM	phase change material
A	ambient
0	initial

**Table 1**

Thermophysical properties of PCM/graphite composite.

Property	Specification
Thermal conductivity	16.6 ( $\text{W m}^{-2} \text{K}^{-1}$ )
Latent heat	123 ( $\text{kJ kg}^{-1}$ )
PCM melting range	42–45 °C
Specific heat	1.98 ( $\text{kJ kg}^{-1} \text{K}^{-1}$ )
Bulk density of composite	789 ( $\text{kg m}^{-3}$ )
Bulk density of graphite	210 ( $\text{kg m}^{-3}$ )

tested by All Cell Technologies LLC in a project co-sponsored by IIT and the City of Chicago. The experimental Li-ion pack consists of 67 modules, each containing twenty commercially available 1.5 Ah Type 18,650 high power cells. Each module consists of five strings of four cells in series with the five strings connected in parallel. The nominal voltage and capacity of each module, shown in Fig. 1, is 14.4 V and 7.5 Ah, respectively.

Paraffin wax can be encapsulated in the graphite matrix to produce a composite with high thermal conductivity and high latent heat storage. The PCM is loaded into the graphite matrix through capillary forces between liquid PCM and the graphite. Table 1 summarizes the characteristics of the PCM/graphite composite used in the battery pack.

### 3. Theory and mathematical modeling

In the passive thermal management system, the heat generated within the cells of a module is transferred to the PCM matrix and then spread by conduction throughout the module. On the other hand, in active cooling the heat generated within the cells is transferred to an air flow maintained (by natural or forced convection)

in the spacing between cells in a module. In both cases, the thermal model assumes that heat transfer within the cells takes place by conduction only, and that heat transfer from the module to the ambient air takes place by convection at the boundary of the module (Fig. 2). The governing equations of each system are summarized as

#### (a) Model equations

##### (i) Air-cooling

Energy balance equation for cell:

$$\rho_c C_p \frac{\partial T_c}{\partial t} = \nabla \cdot (k_c \nabla T_c) + Q(t) \quad (1)$$

##### (ii) PCM cooling

Energy balance equation for cell:

$$\rho_c C_p \frac{\partial T_c}{\partial t} = \nabla \cdot (k_c \nabla T_c) + Q(t) \quad (2)$$

Energy balance equation for PCM block:

$$\rho_{\text{PCM}} C_{p\text{PCM}} \frac{\partial T_{\text{PCM}}}{\partial t} = \nabla \cdot (k_{\text{PCM}} \nabla T_{\text{PCM}}) \quad (3)$$

#### (b) Boundary conditions

##### (i) Air-cooling

$$t = t_0 \quad T = T_0$$

$$\text{BC1 : at } r = R - k_c \frac{\partial T_c}{\partial r} = h(T_c - T_A) \quad (4)$$

$$\text{BC2 : at } r = 0 \frac{\partial T_c}{\partial r} = 0$$

##### (ii) PCM cooling

$$t = t_0 \quad T = T_0$$

$$\text{BC1 - 2 : at } r = R - k_c \frac{\partial T_c}{\partial r} = -k_{\text{PCM}} \frac{\partial T_{\text{PCM}}}{\partial r}$$

$$\text{BC3 : at PCM-air interface } -k_{\text{PCM}} \frac{\partial T_{\text{PCM}}}{\partial t} = h(T_{\text{PCM}} - T_A)$$

$$\text{BC4 : at cell-air interface } -k_c \frac{\partial T_c}{\partial t} = h(T_c - T_A) \quad (5)$$

The set of governing equations was solved numerically using FEMLAB 3.1, a commercial modeling environment that solves partial differential equations simultaneously by applying the finite element method. The model uses differential equations to calculate the temperature in the cell and the PCM matrix. A convection and conduction application mode is used for the energy balance equations.

#### (c) Determination of heat generation during thermal runaway or discharge

The rate of heat generation released during thermal runaway or during discharge was determined by means of an accelerating rate calorimetry (ARC) measurement. The experimental heat

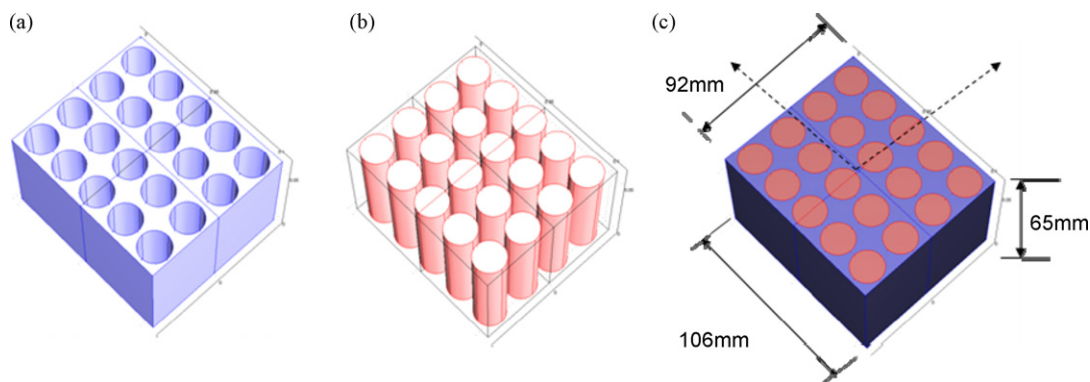


**Fig. 1.** Schematic representation of 5S4P module configuration: (a) PCM filled closed box, (b) Li-ion cells and (c) battery module.

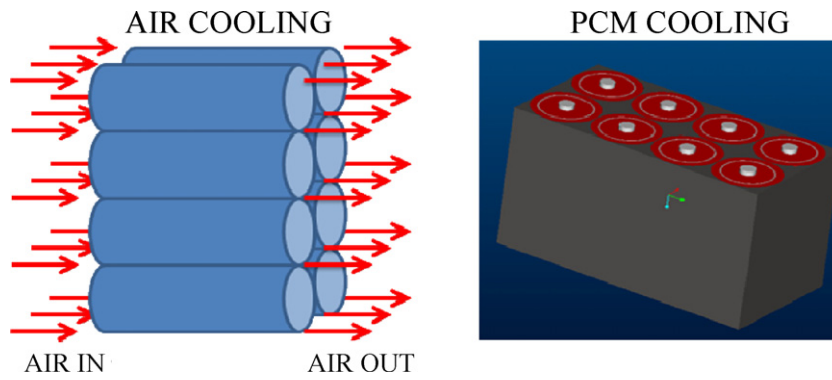


Fig. 2. Representation of active (air) cooling vs. passive (PCM) cooling.

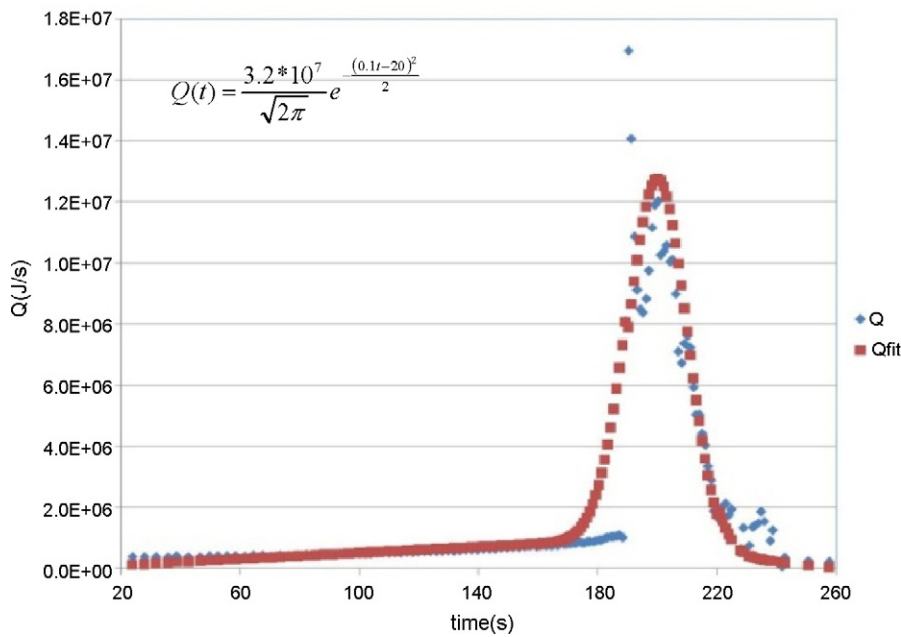


Fig. 3. Rate of heat generation per unit time based on measurements by ARC for Type 18,650 high power cells.

flux during discharge was fit to a polynomial equation whereas the experimental heat flux was fit to a normal curve which the ARC measures as a function of temperature. Fig. 3 shows the thermal runaway data transformed into an expression for the lumped heat generation in a cell as a function of time.

In order to predict the temperature distribution in the module, the heat generated by the runaway reaction or the discharge reactions in an individual cell was then used as a heat source term in an energy balance applied to the module.

#### 4. Results and discussion

##### 4.1. Control of temperature rise

In this part of the study, the temperature history of each cell in a module was modeled for the two cooling modes (active cooling vs. passive cooling by PCM) under abusive discharge conditions. Feller et al. pointed out that lithium-ion cells cycled at ambient temperature with currents greater than 2C can experience an internal temperature of more than 38 °C [8]. Shim et al. presented higher capacity loss at high operating temperature (60 °C) compared to lower operating temperatures [9]. It is clear that both

higher discharge rates and higher operating temperatures have a significant impact on the cell power loss and impedance rise. Fig. 4 presents the average temperature of an interior Li-ion cell during a discharge under stressed conditions ( $T_{amb} = 40\text{ }^{\circ}\text{C}$ , discharge

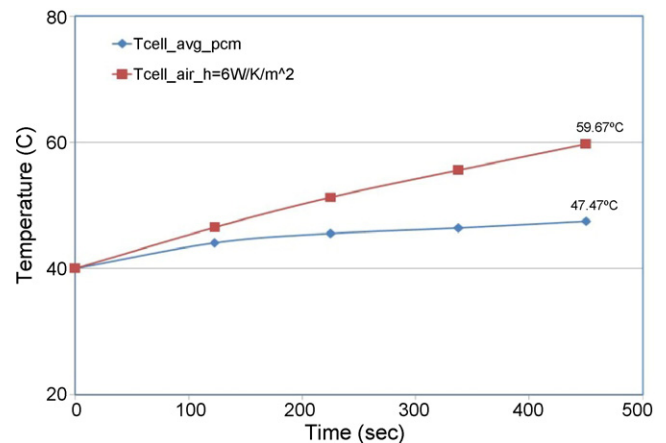


Fig. 4. Cell temperature increase for PHEV-20 battery pack under stressed discharge conditions ( $T_{amb} = 40\text{ }^{\circ}\text{C}$ , discharge rate = 6.67 C, 50 A/module).

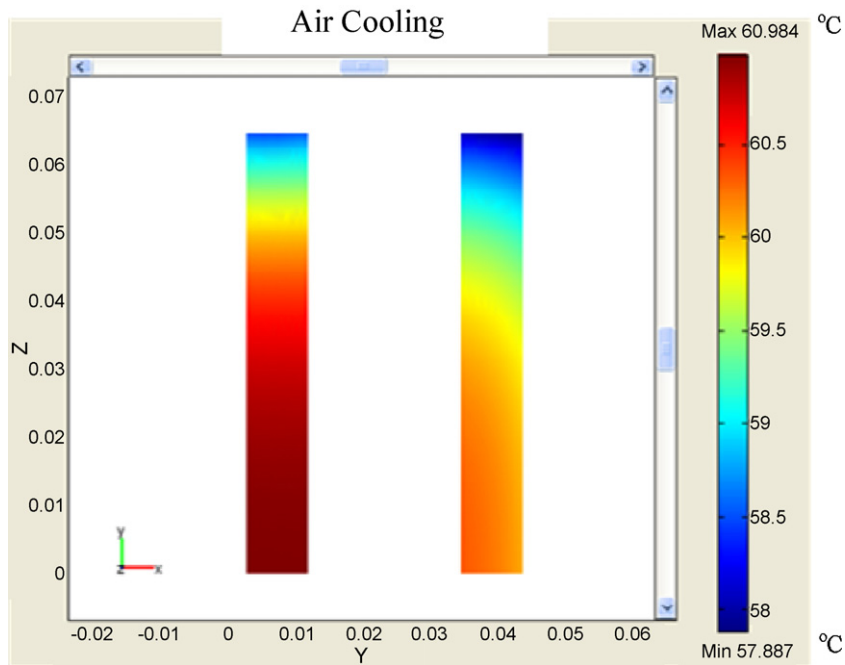


Fig. 5. Temperature profiles in two adjacent cells when air-cooling is applied ( $T_{amb} = 40^\circ\text{C}$ , discharge rate = 6.67 C, 50 A/module).

rate 6.67 C, 50 A/module). With air-cooling, the increase in average temperature of the cell was constant and the temperature reached  $60^\circ\text{C}$  at the end of the discharge. Unfortunately, the operation of most Li-ion cells is limited to a temperature of  $20\text{--}55^\circ\text{C}$ , in which heat generation due to internal resistance and polarization is easily controlled by working with the voltage window and range of charge/discharge rates recommended by the manufacturers. On the other hand, the temperature increase of an interior cell in the PCM-cooled module of a PHEV battery pack reflected the heat absorption by the PCM surrounding the cells in the module. Heat absorption takes place both as sensible heat and as latent heat. When the temperature of the module reaches the melting range of the PCM ( $T_m = 42\text{--}45^\circ\text{C}$ , in this case), the PCM starts to melt and the high

latent heat of the PCM prevents the module temperature from rising sharply (Fig. 4). Note that the average temperature of the cell stays below  $50^\circ\text{C}$  at all times, due to proper design of the PCM matrix and optimal selection of the PCM composition. A detailed work on the comparison of air vs. passive cooling was studied by Sabbah et al. and can be found elsewhere [10].

#### 4.2. Temperature uniformity in-cell and module

Temperature uniformity within a cell, as well as from cell to cell, is important to achieve maximum cycle life (minimum long-term degradation) of cell, module, and pack. The temperature profile along a single cell was studied, assuming near-uniformity in the

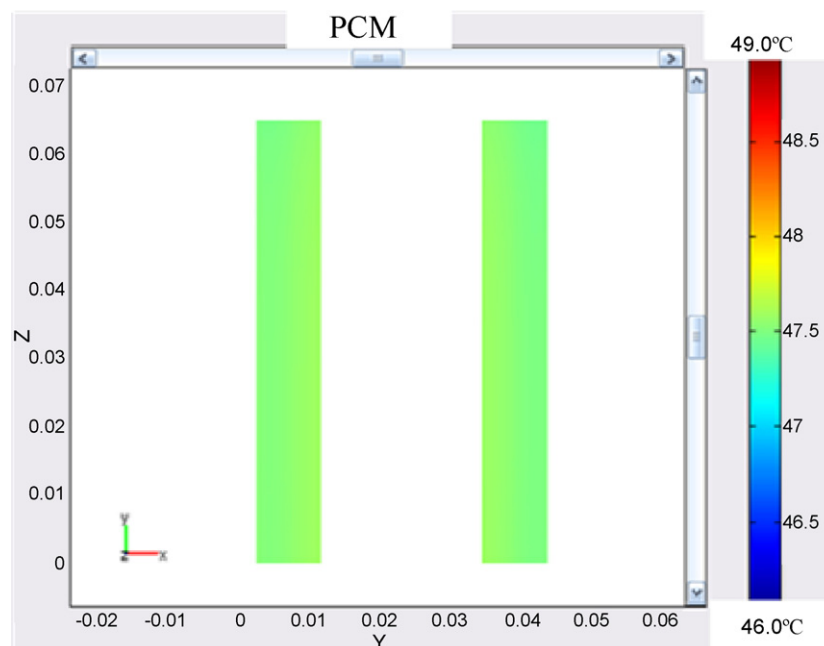


Fig. 6. Temperature profiles in two adjacent cells when passive cooling, is applied by All Cell's PCM matrix ( $T_{amb} = 40^\circ\text{C}$ , discharge rate = 6.67 C, 50 A/module).

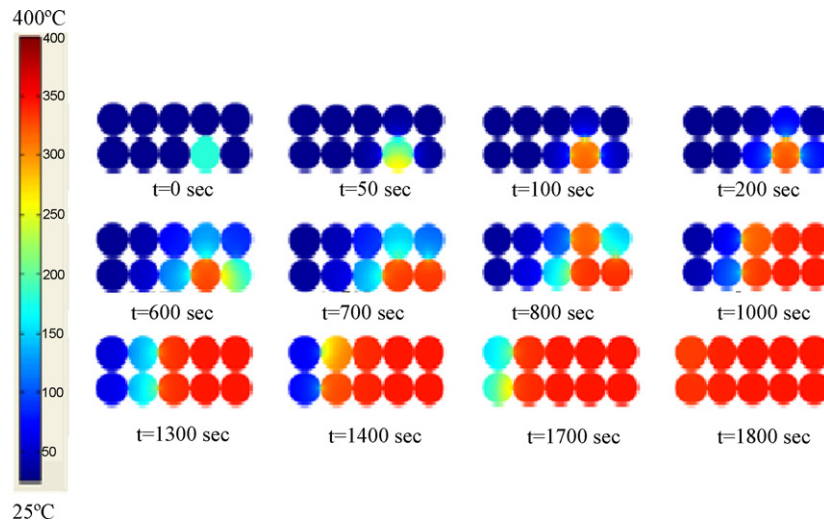


Fig. 7. Propagation of thermal runaway spreading due to a single runaway cell (light blue at  $t=0$ ) in an air-cooled module.

radial direction due to the high aspect ratio of the Type 18,650 cells.

Fig. 5 shows that, with air-cooling, the temperature uniformity in a cell was marginally sufficient under normal discharge conditions. The temperature difference along the cell may be as high as  $3^{\circ}\text{C}$ . As shown in Fig. 5, two adjacent cells have significantly different temperature profiles. Furthermore, the higher the rate of convection, the greater the non-uniformity is. This means that air-cooling does not favor uniformity of the temperature distribution (in-cell as well as cell-to-cell). Non-uniformity of the temperature within a cell will eventually lead to a faster degradation rate and affect the cycle life of the cell. If this happens in a Li-ion pack, it is anticipated that there will be unbalancing between the cells, which will affect the performance drastically. On the other hand, the uniformity of temperature was excellent in the PCM-cooled module and cells. The in-cell temperature profiles were identical in adjacent cells, and the in-cell temperature variation was less than  $0.2^{\circ}\text{C}$  (Fig. 6). The high thermal conductivity of the graphite/PCM matrix insured high rate of the removal of heat and minimized the temperature distribution within the cell. The small temperature difference ( $0.2^{\circ}\text{C}$ ) in adjacent cells also confirms that the heat is conducted efficiently throughout the graphite matrix.

#### 4.3. Prevention of thermal runaway propagation

##### (i) No spacing between cells

To compare the effectiveness of PCM cooling and air-cooling, thermal runaway propagation was modeled for a PHEV module with Type 18,650 cells as discussed above at ambient temperature of  $25^{\circ}\text{C}$ . In the case of air-cooling, the heat transfer coefficient to air flowing through the interstitial spaces of the cells was assumed to be  $10\text{ W m}^{-2}\text{ K}^{-1}$ . Modeling results show that at time  $t=0$ , failure of individual cell (internal short, causing an initial local  $T=180^{\circ}\text{C}$ ) triggers runaway throughout the module if air-cooling is used (Fig. 7). In PCM cooling, the runaway does not propagate and the temperature in the module returns to near-ambient values (Fig. 8). In the latter case, the high thermal conductivity PCM-graphite matrix absorbs and spreads the heat very quickly. Contrary to PCM cooling, the conduction of heat from cell to cell was significantly higher than the heat dissipation through the air.

These results indicate that thermal runaway that occurs accidentally (for example due to a defect) in one individual cell may be prevented from spreading by using a PCM matrix for cooling. Therefore, PCM technology could have a key safety

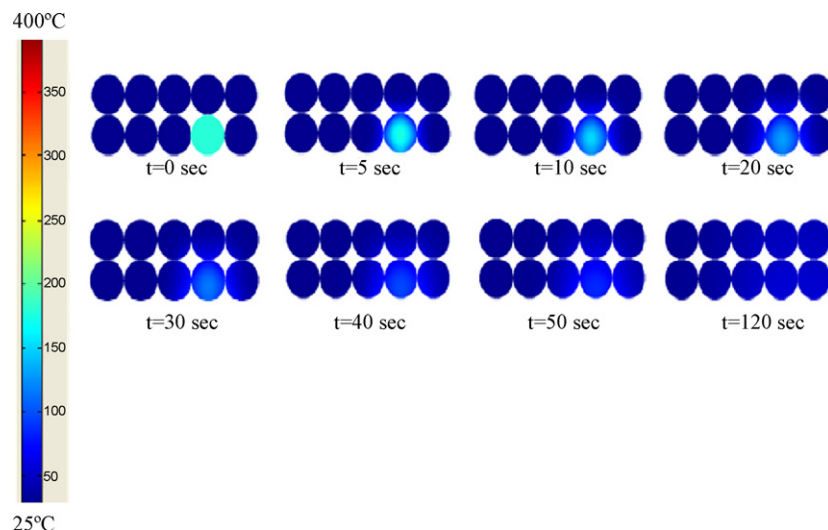


Fig. 8. Propagation of thermal runaway due to a single runaway cell is prevented by interstitial PCM microencapsulated in graphite.

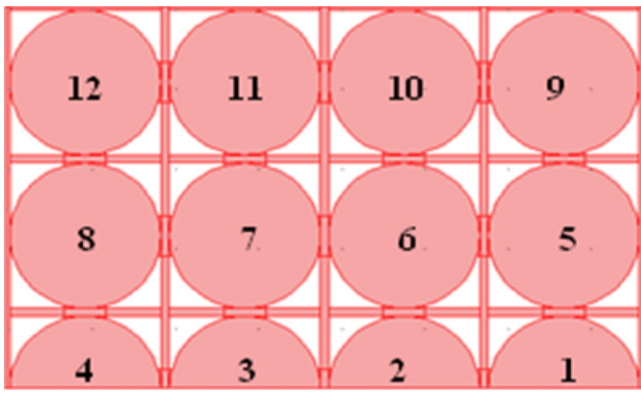


Fig. 9. Top view of the half module with insulating stand.

advantage over conventional air-cooling of compact packs. Initial nail penetration tests in All Cell’s laboratories confirm this conclusion and results will be published soon. Further investigation is underway to see if this advantage holds in other conditions or for larger cells.

(ii) Effect of spacing between cells

Spacing effect was also one of the objectives of this study. It is obvious that spacing between cells eliminates the conduction term between the cells and if the cooling is sufficient enough, the heat will be removed from the system effectively. Since the PCM worked well even without spacing, there is no need to show how the pack with PCM behaves with spacing. However, spacing between cells in a non-PCM pack is dependent on the cooling system. Therefore, the cells are kept 1 and 2 mm apart from each other by placing an insulator (nylon with  $k=0.25 \text{ (W m}^{-2} \text{ K}^{-1})$ ,  $\rho=1140 \text{ (kg m}^{-3})$  and  $C_p=1700 \text{ (J kg}^{-1} \text{ K}^{-1})$  which also works as a stand for the cells. Air flows between the gaps. Fig. 9 represents the top view of a half module. Failure of cell #1 started thermal runaway. Fig. 10a and b shows the cells temperatures versus time for 1 and 2 mm gap, respectively. At  $t=0$ , cell 1 is set to thermal runaway condition which generates a significant amount of heat as shown in Fig. 3. The heat generated by thermal runaway is removed by the air-cooling and also conducted to the other cells through the plastic insulator. It is clearly seen from Fig. 10 that the prop-

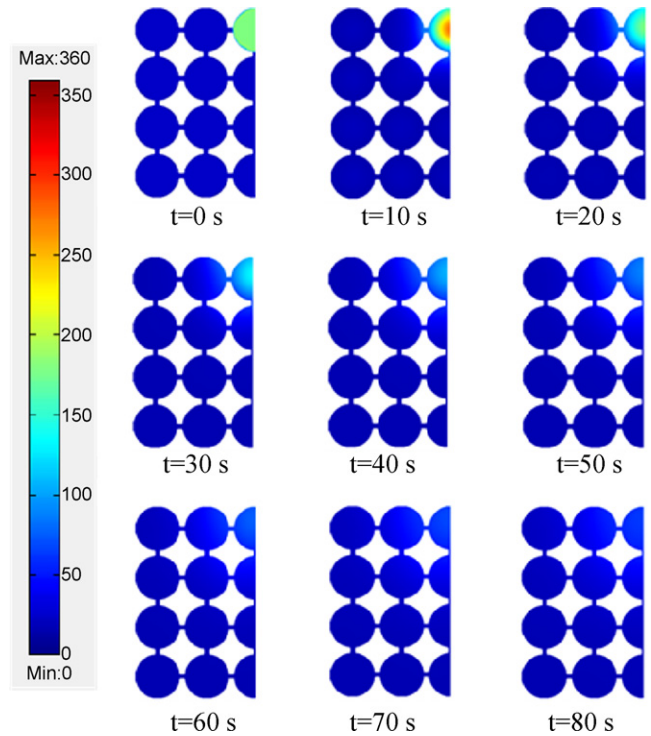


Fig. 11. Propagation of thermal runaway due to a single runaway cell is prevented by interstitial PCM microencapsulated in graphite when nickel interconnections are considered.

agation of the thermal runaway can be prevented by leaving a space between the cells. If the spacing between the cells is 2 mm, temperature of neighboring cells changes only 7 °C during thermal runaway of a cell. On the other hand, when the spacing is 1 mm, the temperature increase is as high as 9.5 °C. The figures also show how cells in direct contact with the triggered cell experience higher temperatures than cells that are not, as for cells 2 and 5. It is clear from Fig. 10a and b that cell 5 showed higher temperatures in both cases despite the fact that both cells are in direct contact with the triggered cell. This observation is caused by the number of cells that are in direct

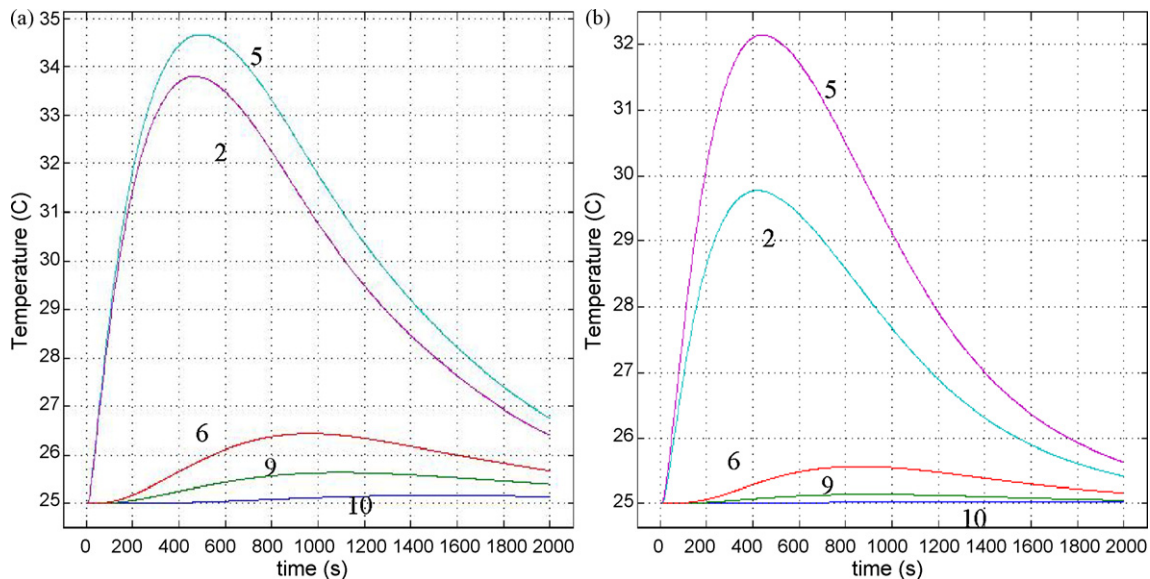
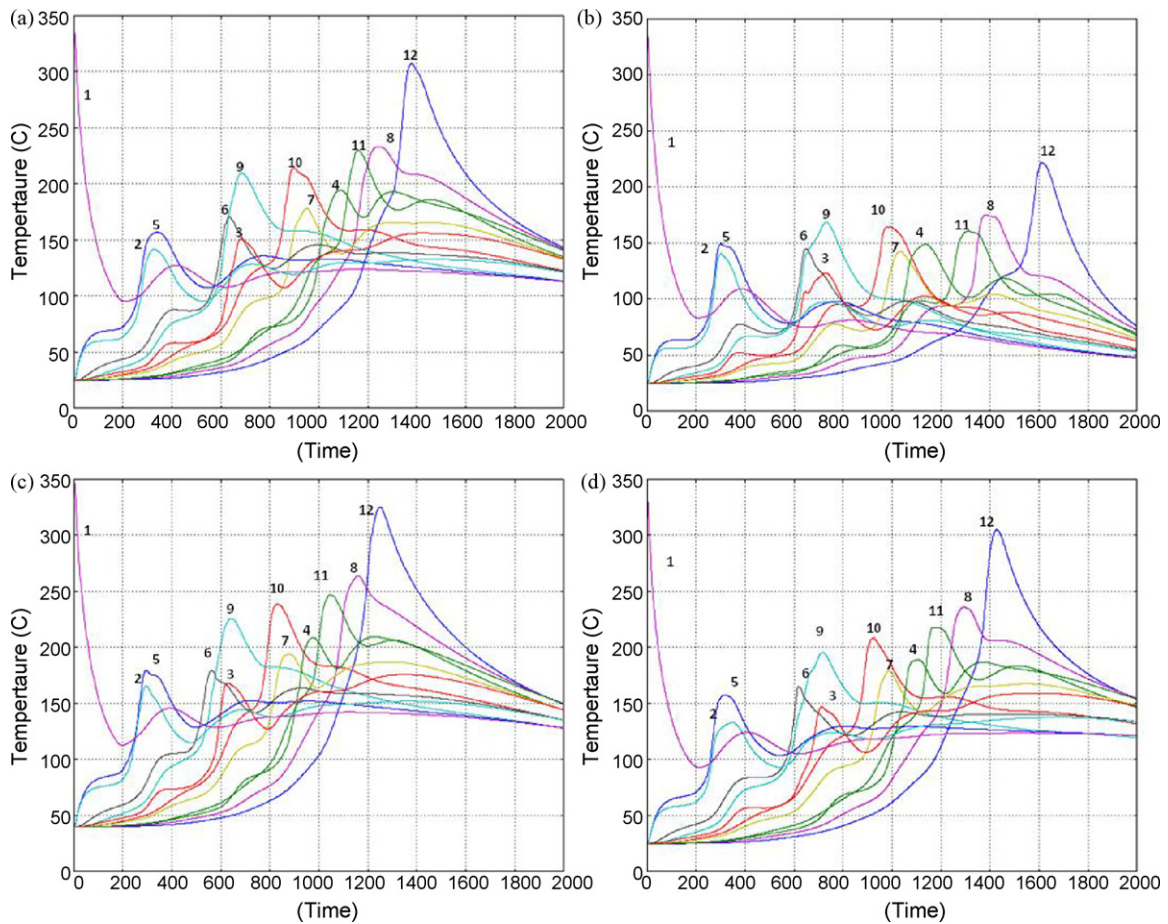


Fig. 10. Temperature profiles of selected points when air is used as cooling: (a) 1 mm spacing between cells and (b) 2 mm spacing between cells.



**Fig. 12.** Temperature profiles of cells during thermal runaway when air is used as cooling: (a) 1 mm gap between cells,  $h = 5 \text{ W m}^{-2} \text{ K}^{-1}$  and  $T_{\text{amb}} = 25^\circ \text{C}$ , (b) 1 mm gap,  $h = 20 \text{ W m}^{-2} \text{ K}^{-1}$  and  $T_{\text{amb}} = 25^\circ \text{C}$ , (c) 1 mm gap,  $h = 5 \text{ W m}^{-2} \text{ K}^{-1}$  and  $T_{\text{amb}} = 40^\circ \text{C}$ , and (d) 2 mm gap,  $h = 20 \text{ W m}^{-2} \text{ K}^{-1}$  and  $T_{\text{amb}} = 25^\circ \text{C}$ .

contact with the cell. For example, cell 5 is in direct contact with three cells including the triggered cell (cell 1), whereas cell 2 is indirect contact with 4 cells including the triggered cell (cell 1). As a result, cell 2 conducts heat to four cells, whereas cell 5 conducts to only three cells which explain the temperature difference between cell 2 and cell 5.

### (iii) Effect of nickel strips

Previous examples of thermal runaway propagations minimize the thermal conductivities between the cells. However, cells are arranged in a series of 4 strings of cells with each string having 5 cells in parallel connected by Ni-strips in order to have electrical connections between cells. These connections behave as thermal bridges as well, in which a significant amount of heat is transferred to neighboring cells. In this part of the work, the effect of described thermal bridges is analyzed in the cases of passive and active cooling.

Fig. 11 shows how the thermal runaway is prevented when PCM/graphite matrix was used as a thermal management system. The heat generated during thermal runaway was properly absorbed by the PCM material in less than 1.5 min and prevented the possible propagation of thermal runaway.

Fig. 12 summarizes the thermal runaway schemes at different conditions when air-cooling is preferred for thermal management. The propagation of thermal runaway at  $T = 25^\circ \text{C}$  and  $h = 5 \text{ W m}^{-2} \text{ K}^{-1}$  was shown in Fig. 12a, and intensity of generated heat increases cell by cell as the propagation proceeds. Under the studied condition, all cells reached the thermal runaway temperature. When the heat transfer coefficient was increased to

$20 \text{ W m}^{-2} \text{ K}^{-1}$ , a majority of the cells kept below  $200^\circ \text{C}$ , but propagation of thermal runaway was still observed in all cells (Fig. 12b). If the ambient temperature was increased to  $40^\circ \text{C}$ , the temperature profiles of each cell was affected linearly when they are compared with the case a. The results show that the major effect of propagation thermal runaway was due to the significant heat release during thermal runaway. However, any increase in ambient temperature will result in corresponding increase in-cell temperature which brings the cell temperature to thermal runaway triggering point earlier as could be seen by comparing Fig. 12a and c. This time advance in thermal runaway triggering due to higher room temperature is not the same for all cells. The thermal runaway time advance accumulates as thermal runaway propagates through the battery pack. For example, cell 2 time advances is 40 s whereas it is more than 100 s for cell 12. The effect of spacing between the cells on thermal runaway was also studied (Fig. 12d). When spacing was doubled from 1 to 2 mm, the propagation of thermal runaway was unavoidable if the cooling was not adequate. The effect of nickel interconnections on heat transfer was significant and triggers the local temperature of a cell. This effect will result in a chain reaction in the cell. The dissipation rate of heat was less than the heat release.

## 5. Conclusion

The advantage of using the PCM thermal management systems over conventional active cooling systems was demonstrated in this study. Thermal modeling of a compact Type 18,650-cell module (4S5P) indicates that a PCM-graphite matrix absorbs and spreads the heat very quickly due to its high thermal conductivity heat

capacity. It is possible to achieve uniform temperature under normal and stressed conditions if the passive thermal management system is used. Contrary to complex cooling systems, the packs with PCM offer safety under stressed conditions. The conduction and absorption of heat by the PCM–graphite matrix prevents propagation of thermal runaway due to a defect in a single cell which has reached runaway condition. PCM technology appears to be an elegant and effective alternative to forced air-cooling of compact packs, and allows a much simplified cooling design for PHEVs. In addition, PCM passive control may make active control, if necessary at all, complementary and/or secondary in function, and therefore leads to a much simplified and more economic design.

### Acknowledgment

The authors are grateful for the financial and technical support provided by All Cell Technologies, LLC (Chicago, IL).

### References

- [1] [http://www.eere.energy.gov/vehiclesandfuels/pdfs/program/fc.fuel\\_partnership\\_plan.pdf](http://www.eere.energy.gov/vehiclesandfuels/pdfs/program/fc.fuel_partnership_plan.pdf), last accessed: 08/06/2007.
- [2] H. Maleki, G. Deng, A. Anani, J. Howard, Thermal stability studies of binder materials in anodes for lithium-ion batteries, *J. Electrochem. Soc.* 146 (1999) 3224–3229.
- [3] S. Al-Hallaj, J.R. Selmán, US Patent 6,468,689 B1, 22 October (2002) Novel Thermal Management of Battery Systems.
- [4] S. Al-Hallaj, J.R. Selmán, US Patent 6,942,944 B2, 13 September (2005) Battery System Thermal Management.
- [5] S. Al-Hallaj, J.R. Selmán, A novel thermal management system for electric vehicle batteries using phase-change material, *J. Electrochem. Soc.* 147 (2000) 3231–3236.
- [6] S. Al-Hallaj, R. Kizilel, A. Lateef, R. Sabbah, M. Farid, R. Selmán, Passive thermal management using phase change material (PCM) for EV and HEV Li-ion batteries, *IEEE Vehic. Power Propuls. Conf.* (2005) 376–380.
- [7] R. Kizilel, A. Lateef, R. Sabbah, M.M. Farid, J.R. Selaman, S. Al Hallaj, Passive control of temperature excursion and uniformity in high-energy Li-ion battery packs at high current and ambient temperature, *J. Power Sources* 183 (2008) 370–375.
- [8] J.P. Fellner, G.J. Loeber, S.S. Sandhu, Testing of lithium-ion 18,650 cells and characterizing/predicting cell performance, *J. Power Sources* 81/82 (1999) 867–871.
- [9] J. Shim, R. Kostecky, T. Richardson, X. Song, K.A. Striebel, Electrochemical analysis for cycle performance and capacity fading of a lithium-ion battery cycled at elevated temperature, *J. Power Sources* 112 (2002) 222–230.
- [10] R. Sabbah, R. Kizilel, J.R. Selmán, S. Al-Hallaj, Active (air-cooled) vs. passive (PCM) thermal management of high power Li-ion packs: limitation of temperature rise and uniformity of temperature distribution, *J. Power Sources* 182 (2008) (2008) 630–638.